Journal of Power Sources 195 (2010) 1207–1210

Contents lists available at ScienceDirect

Journal of Power Sources

journal homepage: www.elsevier.com/locate/jpowsour

Short communication

Porous NiO/poly(3,4-ethylenedioxythiophene) films as anode materials for lithium ion batteries

X.H. Huang, J.P. Tu*, X.H. Xia, X.L. Wang, J.Y. Xiang, L. Zhang

Department of Materials Science and Engineering and State Key Laboratory of Silicon Materials, Zhejiang University, Zheda Road, No. 38, Hangzhou 310027, China

ARTICLE INFO

Article history:
Received 7 July 2009
Received in revised form 23 August 2009
Accepted 24 August 2009
Available online 31 August 2009

Keywords:
Nickel oxide
Poly(3,4-ethylenedioxythiophene)
Composite film
Anode
Lithium ion battery

ABSTRACT

NiO/poly(3,4-ethylenedioxythiophene) (PEDOT) films are prepared by chemical bath deposition and electrodeposition techniques using nickel foam as the substrate. These composite films are porous, and constructed by many interconnected nanoflakes. As anode materials for lithium ion batteries, the NiO/PEDOT films exhibit weaker polarization and better cycling performance as compared to the bare NiO film. Among these composite films, the NiO/PEDOT film deposited after 2 CV cycles has the best cycling performance, and its specific capacity after 50 cycles at the current density of 2 C is 520 mAh g^{-1}. The improvements of these electrochemical properties are attributed to the PEDOT, a highly conductive polymer, which covers on the surfaces of the NiO nanoflakes, forming a conductive network and thus enhances the electrical conduction of the electrode.

1. Introduction

3d transition-metal oxide (MO, M = Fe, Co, Ni, and Cu) films are widely investigated as anode materials for film lithium ion batteries since they were proposed by Tarascon's team [1–6]. These films exhibit high capacities over 700 mAh g^{-1} even at high charge–discharge current density. However, for many bare films, their capacities reduce very quickly during the repeated discharge–charge cycling. The main reason for this is that these 3d transition-metal oxides are a kind of semiconductor with poor conductivity. To overcome this problem, forming composite with other highly conductive materials such as silver, nickel, carbon, and some conducting polymers is an effective method [7–13].

Poly(3,4-ethylenedioxythiophene) (PEDOT) is a conductive polymer and it can be used to improve the electrochemical performances of electrode materials for lithium ion batteries [14]. In this present work, porous NiO/PEDOT composite films were deposited on the nickel foam substrate. The nickel foam substrate has much larger surface area than the metal-foil flat substrate and much more active materials can be obtained [15,16]. The porous films were constructed by many interconnected NiO nanoflakes and the PEDOT covered on the surfaces of each flake. This porous structure offers a larger electrode/electrolyte contact area and a shorter diffusion length of lithium ions. The PEDOT facilitated the electron transfer between the film, the current collector, and the electrolyte and thus improved the electrochemical properties.

2. Experimental

NiO/PEDOT films were deposited by two steps. Firstly, NiO films were deposited on the nickel foam substrate using chemical bath deposition method as reported in Refs. [17,18]. The solution for chemical bath deposition contained 40 mL of 1 mol L^{-1} $NiSO_4$, 30 mL of 0.25 mol L^{-1} $K_2S_2O_8$, 10 mL of concentrated aqueous ammonia, and 20 mL of deionized water. After depositing for 1 h at room temperature, the films were calcined in a tube furnace at 350 °C for 2 h in flowing argon. Secondly, PEDOT was deposited on the NiO films using electrodeposition technique. The electrolyte was an acetonitrile solution containing 10 mmol L^{-1} of 3,4-ethylenedioxythiophene (EDOT) and 100 mmol L^{-1} of $LiClO_4$. The deposition of PEDOT was performed on a CHI660C electrochemical workstation by a cyclic voltammetry (CV) technique at a sweep rate of 50 mV s^{-1} between 0 and 1.5 V for 1, 2 and 3 cycles, respectively, and finally swept to 1.5 V, using the NiO films as the working electrode, a saturated calomel electrode as the reference electrode, and a Pt foil as the counter electrode.

The films were characterized by scanning electron microscopy (SEM, FEI Sirion-100) and Fourier transform infrared spectrometry (FTIR, Thermo Nicolet-380).

Test cells were assembled in a glove box filled with argon using the NiO or NiO/PEDOT film as the working electrode, Li foil as the counter electrode, and polypropylene film as the separator. The

* Corresponding author. Tel.: +86 571 87952573; fax: +86 571 87952856.
E-mail address: tujp@zju.edu.cn (J.P. Tu).

0378-7753/$ – see front matter © 2009 Elsevier B.V. All rights reserved.
doi:10.1016/j.jpowsour.2009.08.062

electrolyte was a mixed solution containing ethylene carbonate and diethyl carbonate, in which dissolved 1 mol L^{-1} of $LiPF_6$. The cells were galvanostatically discharged and charged at the current density of 2 C (the theoretical capacity of NiO is 718 mAh g^{-1}, which is calculated from the chemical equation: $NiO + 2Li = Ni + Li_2O$, so 1 C = 718 mA g^{-1}) over a voltage of 0.02–3.0 V vs. Li^+/Li. CV tests were carried out using the CHI660C at a scanning rate of 0.5 mV s^{-1} between 0 and 3 V.

3. Results and discussion

Fig. 1 shows the SEM images of the bare NiO film and the NiO/PEDOT films deposited after 1, 2 and 3 CV cycles, respectively. The bare NiO film is porous, and it is constructed by many interconnected NiO nanoflakes, whose thicknesses are about 20 nm. These nanoflakes grow vertically on the substrate, forming a net-like structure and the pores among the flakes are about 200 nm (Fig. 1a). Obviously, this porous film has a large electrode/electrolyte contact area, and during the electrode reaction, the diffusion length of lithium ions in the film is very short, resulting in fast electrochemical reaction and thus obtaining good rate performances. It can be seen that the nanoflakes become thicker after the deposition of PEDOT (Fig. 1b–d). For the film deposited after 3 CV cycles, most of the pores are filled (Fig. 1d).

The comparison of cycling performance of the bare NiO film and three NiO/PEDOT composite films is given in Fig. 2. All of the electrodes were tested in 0.02–3.0 V using the current density of 2 C. For bare NiO film, its specific capacity after 50 cycles is only 340 mAh g^{-1}. However, all of the composite films exhibit enhanced cycling performances. It can be seen that the film prepared after 2 CV cycles has higher reversible capacity and better cycling properties. Its capacity after 50 cycles is 520 mAh g^{-1}, higher than 470 and 450 mAh g^{-1} for the films prepared after 1 and 3 CV cycles. Because of its best electrochemical performance, this film is studied further.

The FTIR spectrum of the NiO/PEDOT composite film prepared after 2 CV cycles is shown in Fig. 3. The peak at 3430 cm^{-1} is ascribed to –OH group of the adsorbed water. The peak at 2930 cm^{-1} is associated with the stretching vibration of CH_2 in the dioxyethylene bridge, and the one at 2350 cm^{-1} is associated to the adsorbed CO_2. The peak at 1630 cm^{-1} corresponds to the bending vibration of –OH group of water, and the one at 1510 and 1330 cm^{-1} relates to the stretching vibration of C=C and C–C in thiophene ring, respectively. The peak at 1100 cm^{-1} is assigned to the stretching vibration of C–O–C in the ethylene dioxy group. The peaks at 970, 830, and 630 cm^{-1} are due to C–S stretching vibration in the thiophene ring [19–22]. A peak characteristic of NiO at 440 cm^{-1} is also observed.

Fig. 4 shows the first discharge/charge curves at the current density of 2 C of bare NiO and NiO/PEDOT film electrodes. Both of two electrodes show the first discharge capacities of about 1000 mAh g^{-1}, higher than the theoretical value (718 mAh g^{-1}), and the first charge capacities of about 600 mAh g^{-1}, leading to the initial columbic efficiency of about 60%. The extra discharge capacities are due to the formation of solid electrolyte interphase (SEI). This SEI layer is a gel-like film which contains ethylene oxide based oligomers, LiF, Li_2CO_3 and lithium alkyl carbonate ($ROCO_2Li$) [23]. It can be seen that the discharge/charge curves for the two electrodes are similar. During the first discharge, the sloping voltage range appears around 1.0–0.5 V, followed a plateau appeared at about 0.5 V, and during the first charge, the curve exhibits two sloping voltage ranges around 1.8 and 2.3 V. Both of the curves exhibit serious hysteresis, but for the NiO/PEDOT film, the hysteresis reduced a little because the PEDOT enhanced the conductivity.

Cyclic voltammetry is often used to study the discharge/charge mechanism of transition-metal oxides used as the anode materials for lithium ion batteries. In the present work, comparison of

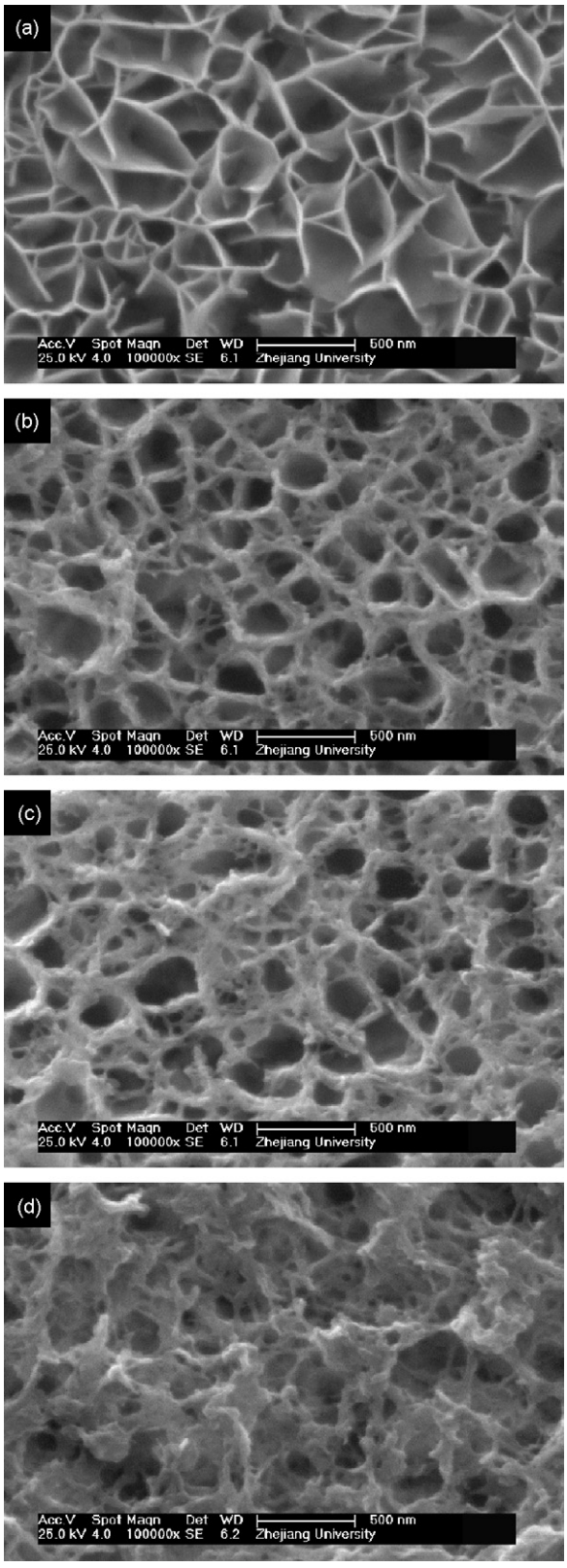

Fig. 1. SEM images of (a) bare NiO and the NiO/PEDOT films prepared after (b) 1, (c) 2, and (d) 3 CV cycles.

CV curves of bare NiO film and NiO/PEDOT composite film prepared after 2 CV cycles are shown in Fig. 5. For the bare NiO film electrode, the two reduction peaks locate at 0.57 and 1.23 V, and they are related to the formation of the solid electrolyte interphase (SEI) layer and the reaction of NiO into Ni [3,4,24–28]. The oxidation

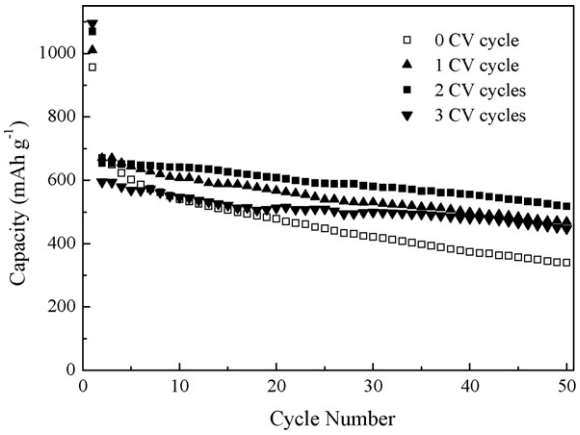

Fig. 2. Cycling performances of bare NiO film (0 CV cycle) and the NiO/PEDOT films prepared after 1, 2, and 3 CV cycles at the current density of 2 C (1 C = 718 mA g^{-1}).

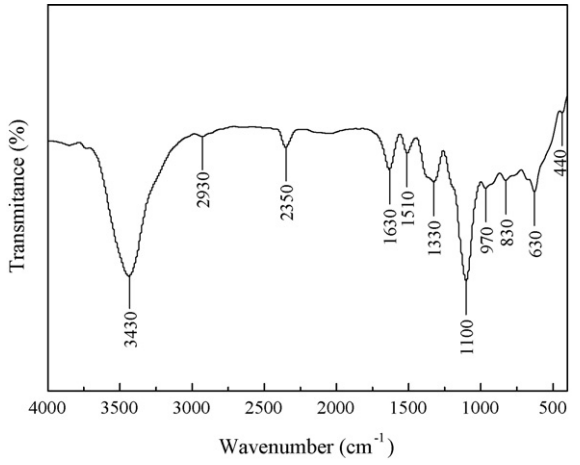

Fig. 3. FTIR spectrum of the NiO/PEDOT composite film prepared after 2 CV cycles.

peaks around 0.75 and 1.82 V are associated with the partial decomposition of the SEI layer, and another oxidation peak at 2.54 V is due to the decomposition of Li_2O [3,4]. For the NiO/PEDOT composite film, the two reduction peaks locate at 1.26 and 0.70 V, and the three oxidation peaks locate at 0.72, 1.72, and 2.45 V, respectively. It can be seen that the separations between the reduction and oxidation peaks decrease for the NiO/PEDOT composite film, indicating a reduced polarization and better reversibility. This is because the

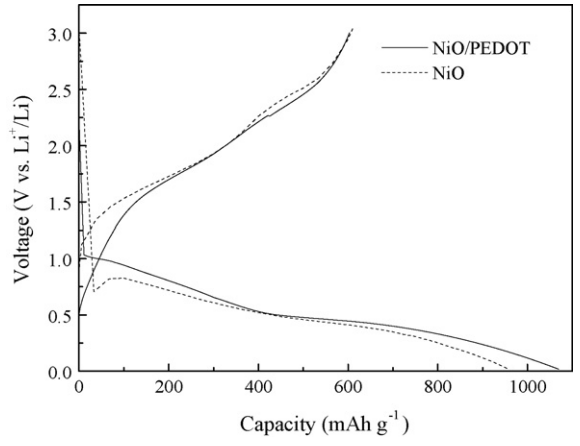

Fig. 4. The first discharge/charge curves at the current density of 2 C of bare NiO and the NiO/PEDOT film prepared after 2 CV cycles.

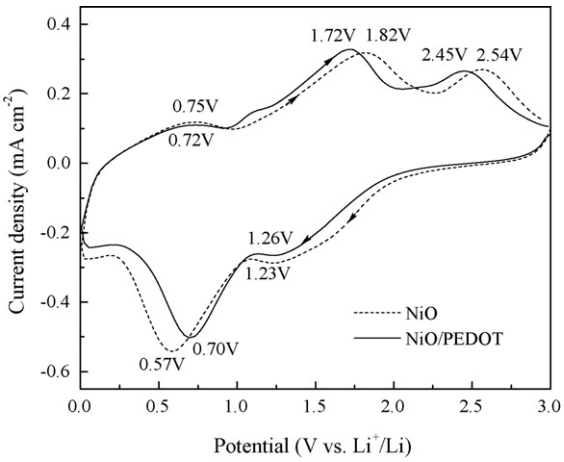

Fig. 5. Comparison of CV curves of bare NiO and the NiO/PEDOT film prepared after 2 CV cycles.

conductive PEDOT enhanced the electrical contact between the NiO flakes, the substrate, and the electrolyte within the electrode.

The better cycling performances of NiO/PEDOT composite films are attributed to their better conductivity, which is enhanced by the PEDOT layer deposited on the surfaces of NiO nanoflakes. The PEDOT layer can keep each NiO flake electrically connected, and also can offer conductive pathways among the NiO nanoflake, the substrate, and the electrolyte. In addition, PEDOT layer on the surface of NiO flakes may keep these flakes from pulverization and thus keep the porous film undamaged during cycling, which is also beneficial for the cycling performance.

4. Conclusions

Porous NiO/PEDOT composite films were prepared by chemical bath deposition and electrodeposition techniques. These films have a porous net-like morphology, which was constructed by NiO nanoflakes coated by PEDOT. Electrochemical tests showed that the composite film prepared after 2 CV cycles exhibited the best cycling performance and its capacity after 50 cycles at 2 C was 520 mAh g^{-1}. Compared to the bare NiO film, this NiO/PEDOT film exhibited weaker polarization and better cycling performance. PEDOT enhanced the electrical conduction of the electrode and may also keep the porous NiO film stable during the cycling.

References

[1] P. Poizot, S. Laruelle, S. Grugeon, L. Dupont, J.-M. Tarascon, Nature 407 (2000) 496.
[2] J.-M. Tarascon, M. Armand, Nature 414 (2001) 359.
[3] S. Grugeon, S. Laruelle, R. Herrera-Urbina, L. Dupont, P. Poizot, J.-M. Tarascon, J. Electrochem. Soc. 148 (2001) A285.
[4] A. Débart, L. Dupont, P. Poizot, J.-B. Leriche, J.-M. Tarascon, J. Electrochem. Soc. 148 (2001) A1266.
[5] D. Larcher, G. Sudant, J.-B. Leriche, Y. Chabre, J.-M. Tarascon, J. Electrochem. Soc. 149 (2002) A234.
[6] P. Poizot, S. Laruelle, S. Grugeon, J.-M. Tarascon, J. Electrochem. Soc. 149 (2002) A1212.
[7] X.H. Huang, J.P. Tu, Z.Y. Zeng, J.Y. Xiang, X.B. Zhao, J. Electrochem. Soc. 155 (2008) A438.
[8] Q.M. Pan, M. Wang, H.B. Wang, J.W. Zhao, G.P. Yin, Electrochim. Acta 54 (2008) 197.
[9] X.H. Huang, J.P. Tu, Y.Z. Yang, J.Y. Xiang, Electrochem. Commun. 10 (2008) 16.
[10] J.Y. Xiang, J.P. Tu, Y.F. Yuan, X.L. Wang, X.H. Huang, Z.Y. Zeng, Electrochim. Acta 54 (2009) 1160.
[11] L. Wang, Y. Yu, P.C. Chen, D.W. Zhang, C.H. Chen, J. Power Sources 183 (2008) 717.
[12] X.H. Huang, J.P. Tu, C.Q. Zhang, X.T. Chen, Y.F. Yuan, H.M. Wu, Electrochim. Acta 52 (2007) 4177.
[13] X.H. Huang, J.P. Tu, X.H. Xia, X.L. Wang, J.Y. Xiang, Electrochem. Commun. 10 (2008) 1288.

[14] J. Chen, Y. Liu, A.I. Minett, C. Lynam, J. Wang, G.G. Wallace, Chem. Mater. 19 (2007) 3595.
[15] Y. Yu, C.-H. Chen, J.-L. Shui, S. Xie, Angew. Chem. Int. Ed. 44 (2005) 7085.
[16] X.H. Huang, J.P. Tu, X.H. Xia, X.L. Wang, J.Y. Xiang, L. Zhang, Y. Zhou, J. Power Sources 188 (2009) 588.
[17] P. Pramanik, S. Bhattacharya, J. Electrochem. Soc. 137 (1990) 3869.
[18] S.-Y. Han, D.-H. Lee, Y.-J. Chang, S.-O. Ryu, T.-J. Lee, C.-H. Chang, J. Electrochem. Soc. 153 (2006) C382.
[19] H. Mao, X. Lu, D. Chao, L. Cui, Y. Li, W. Zhang, J. Phys. Chem. C 112 (2008) 20469.
[20] L. Zhang, H. Peng, P.A. Kilmartin, C. Soeller, J. Travas-Sejdic, Macromolecules 41 (2008) 7671.
[21] V. Rumbau, J.A. Pomposo, A. Eleta, J. Rodriguez, H. Grande, D. Mecerreyes, E. Ochoteco, Biomacromolecules 8 (2007) 315.
[22] J. Jang, M. Chang, H. Yoon, Adv. Mater. 17 (2005) 1616.
[23] G. Gachot, S. Grugeon, M. Armand, S. Pilard, P. Guenot, J.-M. Tarascon, S. Laruelle, J. Power Sources 178 (2008) 409.
[24] P. Balaya, H. Li, L. Kienle, J. Maier, Adv. Funct. Mater. 13 (2003) 621.
[25] R. Dedryvère, S. Laruelle, S. Grugeon, P. Poizot, D. Gonbeau, J.-M. Tarascon, Chem. Mater. 16 (2004) 1056.
[26] P. Tomczyk, H. Sato, K. Yamada, T. Nishina, I. Uchida, J. Electroanal. Chem. 391 (1995) 133.
[27] P. Tomczyk, M. Mosiałek, J. Obłakowski, Electrochim. Acta 47 (2001) 945.
[28] J.-S. Do, C.-H. Weng, J. Power Sources 159 (2006) 323.